

Kinetics and mechanism of the reaction between 2,3,4,5,6-pentafluorophenylacetonitrile and guanidine-like bases and the structure of the products

Błażej Gierczyk, Grzegorz Schroeder, Piotr Przybylski, Bogumil Brzezinski *

Faculty of Chemistry, A. Mickiewicz University, Grunwaldzka 6, 60-780 Poznań, Poland

Received 17 January 2006; accepted 13 February 2006

Available online 27 March 2006

Abstract

The reactions between the 2,3,4,5,6-pentafluorophenylacetonitrile (PFPA) and such strong N-bases as 7-methyl-1,5,7-triazabicyclo[4.4.0]dec-5-ene (MTBD) and 1,5,7-triazabicyclo[4.4.0]dec-5-ene (TBD) have been studied by UV–vis kinetic, high-resolution LSIMS, ¹⁹F NMR and FT-IR methods. The products of these reactions (compounds **1** and **2** and oligomers) have been isolated and their structures have been studied using the methods mentioned. They have been identified as *ortho* or *para* substituted dimers and a mixture of trimers, tetramers and pentamers of PFPA. All the products are formed in a relatively slow processes described by various low equilibrium constants. The structures of the *ortho* or *para* substituted dimers have been visualized by PM5 semiempirical calculations.

© 2006 Elsevier B.V. All rights reserved.

Keywords: N-base; Guanidines; Fluorinated compounds; Carbanions; Nucleophilic substitution; ¹H NMR; ¹⁹F NMR; FT-IR; Mass spectrometry; PM5 semiempirical calculations

1. Introduction

Fluoroorganic compounds, because of their unique chemical, physicochemical and biological properties have been widely studied and used [1,2].

Amidines such as 1,8-diazabicyclo[5.4.0]undec-7-ene (DBU) or 1,5-diazabicyclo[4.3.0]non-5-ene (DBN) and guanidines such as 1,5,7-triazabicyclo[4.4.0]dec-5-ene (TBD), 7-methyl-1,5,7-triazabicyclo[4.4.0]dec-5-ene (MTBD) belong to very strong N-bases with small nucleophilicity [3–8]. DBU, DBN, TBD and MTBD molecules as a very strong N-bases are very important agents in the deprotonation reactions of weak O–H [8–13], N–H [14–16] and C–H [17–19] acids, whereas when protonated they, except for MTBD, can form homo-conjugated complexes [20]. Furthermore, in our previous papers, we have demonstrated that MTBD can form hydrogen-bonded chains with phenols, biphenols and N–H acids in non-polar aprotic solvents as well as in the solid state [9–13,21,22]. The same is true for TBD but the respective complexes have much more complicated structures, both in the solutions and in the solid state [23–25].

In our previous papers, we have also studied the reactions of fluoronitrobenzenes, fluorochlorobenzenes and fluorobenzoic acids with strong nitrogen bases [26–29]. As a further contribution to these studies in this paper we demonstrate the influence of strong bases (TBD and MTBD) on the generation of carbanion by the abstraction of one proton from the methylene group of 2,3,4,5,6-pentafluorophenylacetonitrile (PFPA) followed by intermolecular nucleophilic substitution of fluorine atom yielded various products. The mechanism of the formation of these products as well as their structures are discussed.

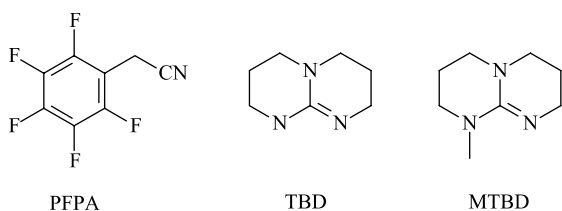
2. Experimental

2,3,4,5,6-Pentafluorophenylacetonitrile and guanidine bases: 1,5,7-triazabicyclo[4.4.0]dec-5-ene (TBD), 7-methyl-1,5,7-triazabicyclo[4.4.0]dec-5-ene (MTBD), and 2,3,4,5,6-pentafluorophenylacetonitrile (PFPA) were commercial products of Fluka and were used without any purification. The structures of these compounds are presented in Scheme 1.

2.1. Synthesis

To a vigorously stirred solution of PFPA (10 mmol) in dry diethyl ether (100 cm³) a solution of MTBD (5 mmol) in the same solvent (25 cm³) was added. The dark violet mixture was heated and stirred for 2 h. After then the solvent was

* Corresponding author. Tel.: +48 61 829 1330; fax: +48 61 865 8008.
E-mail address: bbrzez@main.amu.edu.pl (B. Brzezinski).



Scheme 1. Structures of substrates.

evaporated and the dark, oily residue was dissolved in dichloromethane. This solution was washed twice with 50 cm³ of 1 mol dm⁻³ HCl and the organic layer was separated and dried over Na₂SO₄. The solvent was evaporated in vacuum. The products were separated by column chromatography on silica gel using diethyl ether as eluent. Three fractions were collected: the first (compound **1**), the second (compound **2**) and the third (mixture of oligomers). After solvent evaporation the semisolid products were obtained.

2.2. UV-vis spectra

The UV-vis spectra were recorded in CH₃CN on an Agilent 8453 spectrometer using a 1 cm cell thick and the samples of the concentration 5 × 10⁻⁵ mol dm⁻³. The data of these spectra are collected in Table 1.

2.3. NMR measurements

¹H and ¹⁹F NMR spectra were recorded on Varian-Gemini 300 spectrometer at 300.075 and 282.352 MHz, respectively. The 0.01 M solutions of products in CDCl₃ were used for all measurements. The chemical shifts were measured to an internal standard (TMS for ¹H spectra; CFC₃ for ¹⁹F NMR spectra; δ = 0.000 ppm). For ¹H NMR spectra 60° pulse width 4500 Hz spectral width; 2 s acquisition time; 32k FT-size. The ¹⁹F NMR spectra were measured as follows: spectral width 128k, 60° pulse width and 0.64 s acquisition time.

2.4. FT-IR measurements

The FT-IR spectra of 2,3,4,5,6-pentafluorophenylacetonitrile (PFPA) with MTBD were recorded in acetonitrile (0.10 mol dm⁻³) at 300 K on a Bruker IFS 113v spectrometer. Acetonitrile spectral-grade was stored over 3 Å molecular sieves for several days. All manipulations with the substances were performed in a carefully dried and CO₂-free glove box.

A cell with Si windows and wedge-shaped layers was used to avoid interferences (mean layer thickness 176 μm). The spectra were taken with an IFS 113v FT-IR spectrophotometer (Bruker, Karlsruhe) equipped with a DTGS detector; resolution 2 cm⁻¹, NSS = 125. The Happ-Genzel apodization function was used.

2.5. Mass spectrometry

High-resolution LSIMS spectra were obtained on two sector mass spectrometer (AMD-604) of the B/E geometry using a

Table 1
Elementary analysis and high resolution MS data for negative ions of compounds **1**, **2** and a mixture of oligomers

Compound	Elemental analysis		MS	
	Calc. (%)	Found (%)	Calc.	Found
1	C-48.75	C-48.73	394.0152	393.0079
			C ₁₆ H ₃ F ₉ N ₂	
	H-0.77	H-0.79		
2	N-7.11	N-7.10		
	C-48.75	C-48.73	394.0152	393.0062
			C ₁₆ H ₃ F ₉ N ₂	
Oligomers			580.0119	580.0110
			C ₂₄ H ₃ F ₁₃ N ₃	
			767.0165	767.0174
		C ₃₂ H ₄ F ₁₇ N ₄		
		954.0209	954.0199	
		C ₄₀ H ₅ F ₂₁ N ₅		

peak matching technique and *m*-nitrobenzyl alcohol as solvent. Elemental compositions of the ions discussed were determined with an error less than 10 ppm in relation to perfluorokerosene at a resolving power of 10,000.

2.6. Kinetic measurements

The kinetic runs were carried out using a stop Agilent 8453 spectrophotometer with the cell block thermostated to ±0.1 °C. The kinetic runs were completed under pseudo-first-order conditions with the base concentration in large excess (0.01–0.05 mol dm⁻³). The base solutions were prepared directly before starting the kinetic measurements. The observed rate constants (*k*_{obs}) were calculated from the traces of absorbance vs. time using two methods: intermediate decay (Guggenheim's method) and the formation of the respective newest intermediates (initial rate method). The second-order rate constants for forward (*k*) reaction were calculated by linear least-squares fit of the variation of *k*_{obs} vs. base concentration (*k*_{obs} = *k*[B] + int).

2.7. PM5 calculations

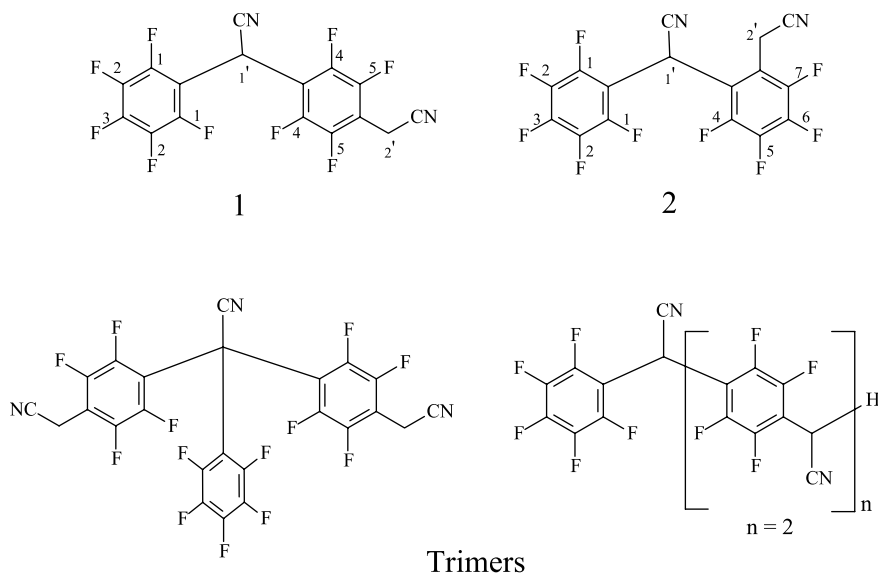
PM5 semiempirical calculations were performed using the WIN MOPAC 2003 program [30]. The full geometry optimization was carried out without any symmetry constraints [31].

2.8. Elementary analysis

The elementary analysis was carried out on Vario ELIII (Elementar, USA).

3. Results and discussion

The formulae and the atoms numbering in the compounds obtained (**1** and **2** and oligomers) are shown in Scheme 2.



Scheme 2. Structures and atom numbering of compounds **1** and **2** as well as a tetrahedral and linear forms of *para* substituted trimers.

In the reaction, of PFPA with the TBD or MTBD strong bases two dimeric (compounds **1** and **2**) and a mixture of oligomeric products were isolated. The analytical and LSIMS data of these compounds are collected in Table 1. The LSIMS data in this table indicate directly that compounds **1** and **2** are dimers and the other one are mixture of tri-, tetra- and pentamers as indicated in Scheme 2.

The structures of compounds **1** and **2** can be deduced from their ^{19}F NMR spectra. The spectrum of compound **1** shows three signals originated from C_6F_5 - group and two from *para*-substituted $-\text{C}_6\text{F}_4-$ group. In the spectrum of compound **2**, besides the three signals originated from C_6F_5 - group, the *ortho*-substitution is indicated by the presence of four signals attributed to non-equivalent fluorine atoms. Furthermore, all of these signals show the spin–spin coupling with one or two fluorine atoms via three bonds, which is only possible for *ortho*-substituted isomer (Table 2).

3.1. Kinetic studies

In the UV spectrum, of PFPA in acetonitrile a band at $\lambda_{\text{max}} = 242$ nm is observed. After addition of TBD or MTBD, the intensity of this band decreases and a new one arises with $\lambda_{\text{max}} = 310$ nm. This process is very fast but it is characterized by a relatively low equilibrium constant. With time the concentration of this intermediate decreases and a new one characterized by $\lambda_{\text{max}} = 440$ nm appears. The newly formed intermediate converts into another ($\lambda_{\text{max}} = 390$ nm) and finally into a product with $\lambda_{\text{max}} = 250$ nm. It is interesting to note that an addition of HCl to neutralize the solution containing the intermediate, for which $\lambda_{\text{max}} = 390$ nm is observed, changes the direction of all reactions with the formation of the substrate ($\lambda_{\text{max}} = 242$ nm) indicating that all these reactions are reversible. The reaction pathway and the structures of the intermediates characterized by respective λ_{max} are shown in

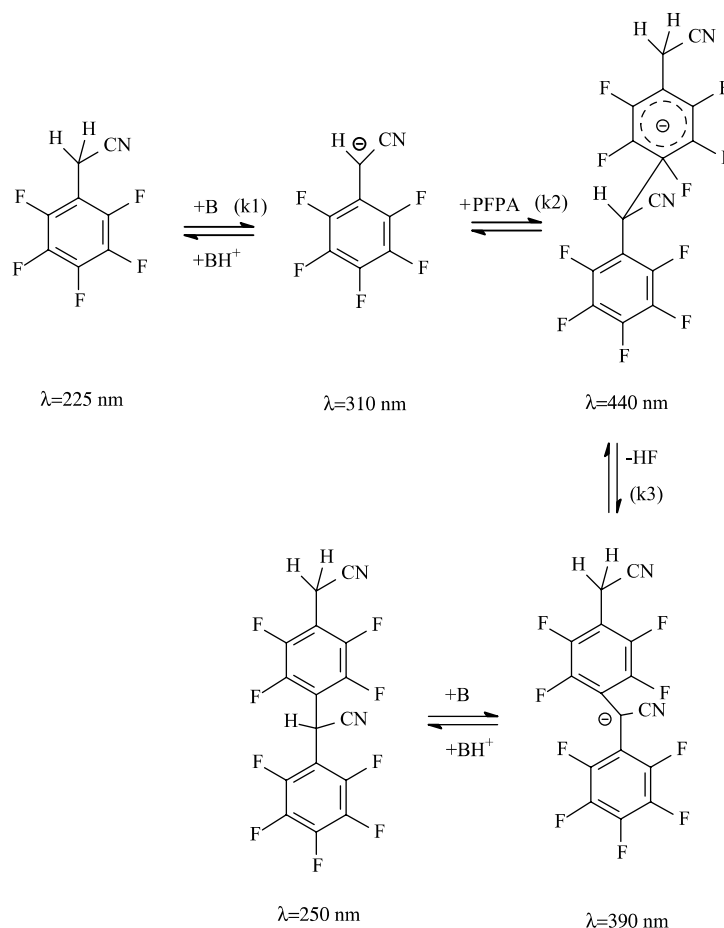
Table 2
Spectral data for compounds obtained

Compound	HR-MS neg. ion	^1H NMR (ppm)		^{19}F NMR (ppm)						
		1'	2'	1	2	3	4	5	6	7
1	393.0079	4.52; 1H s	3.89; 2H s	−143.7; 2F d; 22 Hz	−165.8; 2F t; 22 Hz	−170.5; 1F t; 22 Hz	−145.7; 2F d; 21 Hz	−148.2; 2F d; 21 Hz	–	–
2	393.0062	4.61; 1H s	3.85; 2H s	−142.7; 2F d; 22 Hz	−166.3; 2F t; 22 Hz	−170.2; 1F t; 22 Hz	−146.3; 1F d; 20 Hz	−168.4; 1F t; 20 Hz	−168.9; 1F t; 20 Hz	−147.4; 1F d; 20 Hz
Oligomers (mixture)	580.0110; 767.0174; 954.0199 ^a	4.6; b	3.8–3.9; b	−142.7; −143.9; −144.5; −145.5; −147.4; −147.9; −165.0; −166.4; −166.9; −167.3; −168.5; −170.3; −170.7 ^b						

s, singlet, d, doublet; t, triplet; b, broad signal.

^a Only main peaks were noted.

^b All signal were broadened.



Scheme 3. Proposed mechanism of the reaction of PFPA with N-bases (*para* substitution is shown as an example).

Scheme 3 and the rate constants determined are collected in Table 3. Except for the reaction of the formation of the intermediate with $\lambda_{\text{max}}=310 \text{ nm}$ all the reactions are rather slow.

3.2. FT-IR studies

Recently, we have discussed the FT-IR spectra of MTBD and its protonated forms in acetonitrile [10]. The spectrum of MTBD is characterised by the so-called Bohlmann band at 2846 cm^{-1} and the $\nu(\text{C}=\text{N})$ vibrations at 1609 cm^{-1} . When MTBD is protonated, the band assigned to the $\nu(\text{N}^+\text{H})$ vibration arises at 3377 cm^{-1} and the $\nu(\text{C}=\text{N})$ vibrations appear as an intense doublet with maxima at 1627 and 1602 cm^{-1} if the protonated MTBD cation is non-hydrogen bonded.

Fig. 1(a–c) shows the FT-IR spectra in the region $4000\text{--}400 \text{ cm}^{-1}$ of the acetonitrile mixtures of PFPA and MTBD with different ratios. For comparison, the spectrum of MTBD is also given. In Fig. 2(a–c), the regions of the Bohlmann bands, the stretching vibrations of cyano groups $\nu(\text{C}\equiv\text{N})$ and the $\nu(\text{C}=\text{N})$ vibrations are given on extended scale.

In the spectrum of the 1:1 mixture of PFPA with MTBD in comparison with that of MTBD the Bohlmann band intensity decreases and instead new bands arise. First of all, a band at 3377 cm^{-1} of a weak intensity as well as a shoulder at 1627 cm^{-1} indicate the presence of protonated and non-hydrogen bonded MTBD molecules. Furthermore, the new band at 2143 cm^{-1} assigned to the $\nu(\text{C}\equiv\text{N})$ vibrations indicates that the cyano group is bonded in the arrangement in which the electron density strongly increases, i.e. in the respective carbanion (intermediate with $\lambda_{\text{max}}=310 \text{ nm}$,

Table 3
Second order rate constants at 25°C [$k \pm \text{SD}$ ($\text{M}^{-1} \text{s}^{-1}$)] for the reactions of PFPA with TBD and MTBD

Kind of rate constant	TBD	MTBD
Product decay $\lambda=310 \text{ nm}$	0.0632 ± 0.0003	0.0055 ± 0.0003
Formation product $\lambda=440 \text{ nm}$	0.0638 ± 0.0004	0.0056 ± 0.0004
Product decay $\lambda=440 \text{ nm}$	0.0327 ± 0.0003	0.0021 ± 0.0002
Formation product $\lambda=390 \text{ nm}$	0.0318 ± 0.0002	0.0021 ± 0.0003

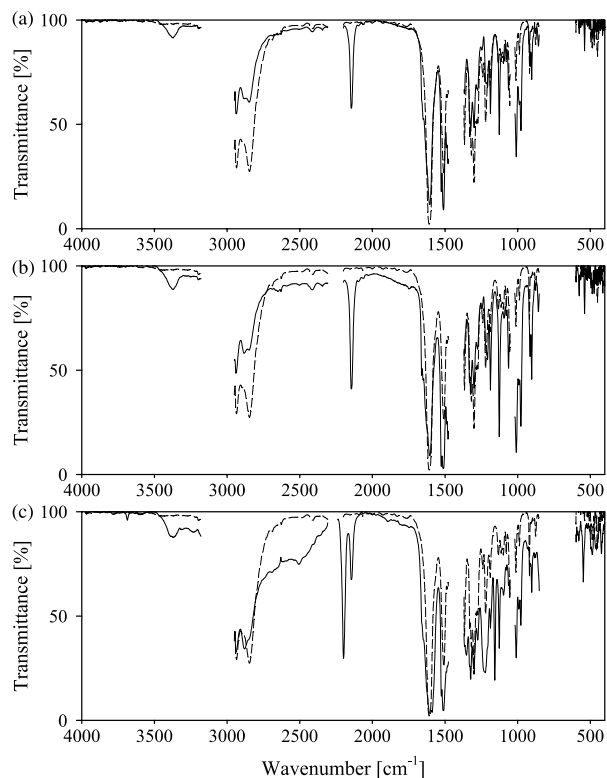


Fig. 1. FT-IR spectra of the mixtures in acetonitrile of PFPA with MTBD (—) and for comparison of MTBD (---): (a) mixture 1:1, (b) mixture 2:1, and (c) mixture 1:2.

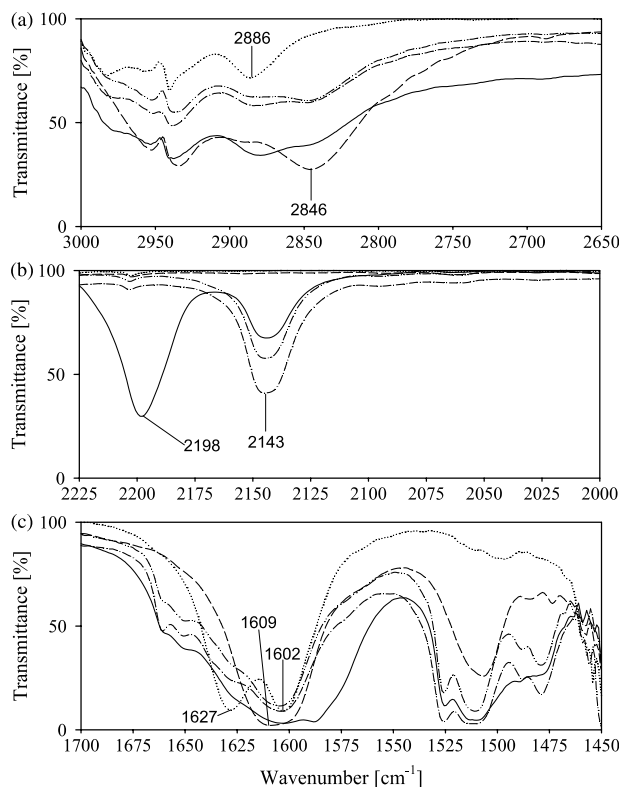
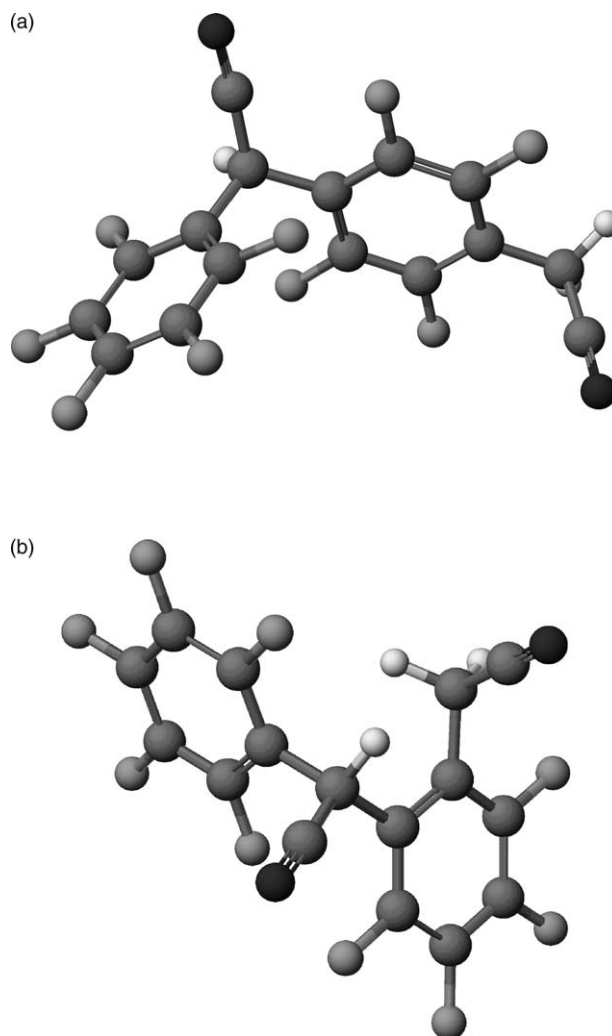


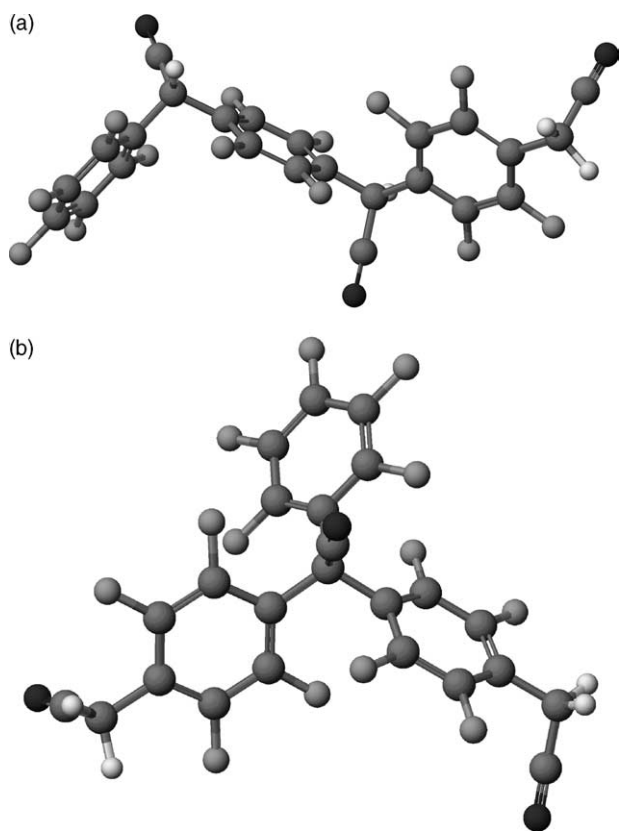
Fig. 2. FT-IR spectra with the extended scales of the mixtures in acetonitrile of PFPA with MTBD of the mixtures: (· · · · · · · · · ·) 1:1, () 2:1, (---) mixture 1:2 (—), and for comparison of MTBD (---) and its protonated form by HAuCl₄ (· · ·).

Scheme 3). It is interesting to note that in the spectrum of the acetonitrile solution of PFPA the respective ν (C≡N) vibrations are masked by the cyano group of the solvent. In the spectrum of the 2:1 mixture of PFPA with MTBD, the intensity of the band of ν (C≡N) vibrations at 2143 cm^{-1} slightly increases due to the shift of the equilibrium reaction with the formation of the carbanion toward the right hand side.

In contrast to the last spectrum, in the spectrum of the 1:2 mixture of PFPA with MTBD, the intensity of the band at 2143 cm^{-1} slightly decreases and a new one much stronger than the first one arises at 2198 cm^{-1} . The position of this new band demonstrates the decrease in the electron density in the arrangement of the cyano group. This observation can be explained by the further reaction of the carbanion with formation of the intermediate with $\lambda_{\text{max}}=390\text{ nm}$ (Scheme 3). It is interesting to note that comparable shifts of the cyano group band position in the FT-IR spectra were earlier observed for the hydrogen bonded complexes of 4-cyanophenol with strong N-bases [9,32]. The structure of intermediate with $\lambda_{\text{max}}=390\text{ nm}$ is further confirmed by the band with a maximum at about 2500 cm^{-1} in the spectrum of 1:2 mixture



Scheme 4. The energetically favorable structures of: (a) compound 1 and (b) compound 2.



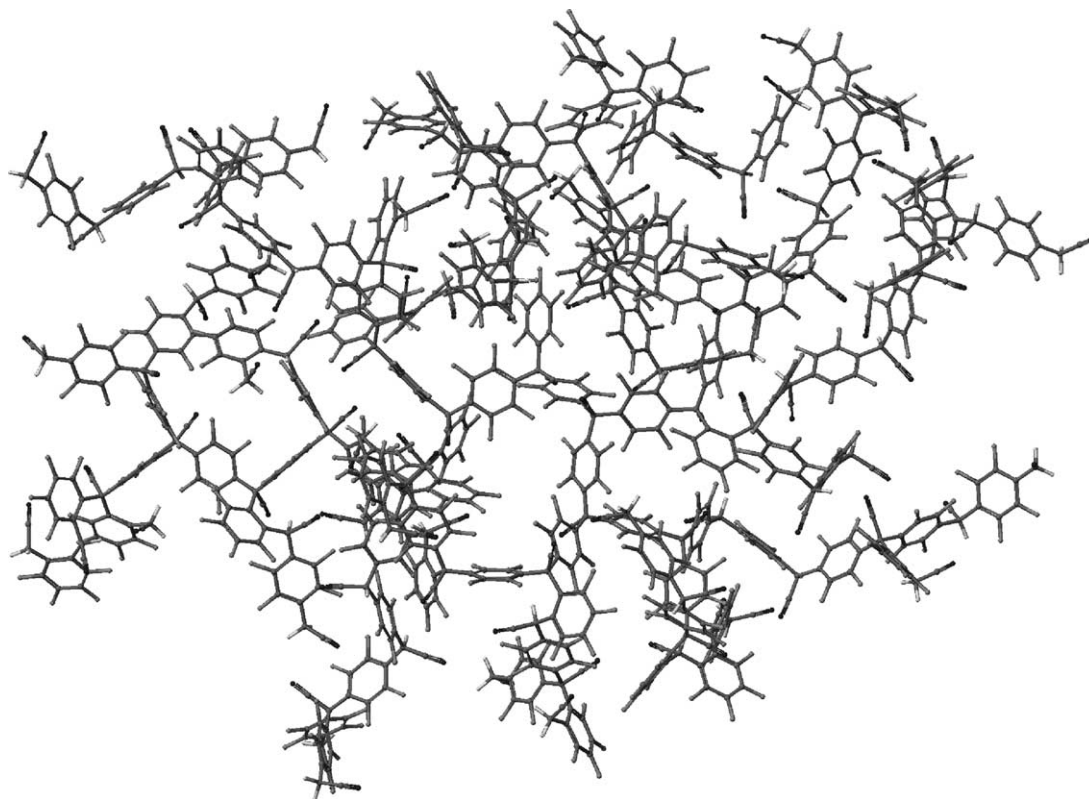
Scheme 5. The energetically favorable structures of trimers: (a) linear and (b) tetrahedral.

of PFPA with MTBD indicating the abstraction of the F^- anion from the 2,3,4,5,6-pentafluorophenyl ring and the formation of an asymmetric $MTBD-H^+ \cdots F^-$ intermolecular hydrogen bond. Furthermore, the presence in the spectrum of the band assigned to the $\nu(N^+H)$ vibration at 3377 cm^{-1} indicates that this F^- anion abstraction process is very slow and it is described by a further equilibrium reaction.

In the spectra of PFPA with MTBD at different ratios in the region $1700\text{--}1450\text{ cm}^{-1}$ (Fig. 2(c)) the bands assigned to the $\nu(C=C)$ aromatic ring vibrations at 1662 , 1526 , 1513 cm^{-1} , characteristic of PFPA molecule, are still observed. Besides these bands, a new bands arise at 1650 cm^{-1} and in the range $1500\text{--}1475\text{ cm}^{-1}$, indicating only partial deprotonation of the PFPA molecule. This also means that the equilibrium constants of the reactions are very low.

3.3. PM5 calculations

The visualized structures of compounds **1** and **2** are shown in Scheme 4. The calculated heats of formation of these favourable structures are -272.82 and -269.34 kcal/mol , respectively. These values demonstrate that both structures are energetically comparable and this can be the reason for their formation under experimental conditions. The structures of isomeric trimers are shown in Scheme 5. The heats of formation of the linear and tetrahedral structures are -390.43 and -384.23 kcal/mol , respectively, indicating that the first one is energetically more favourable. This difference can be probably a result of the stereochemical reason between



Scheme 6. The structure of calculated dendrimer by PM5 method (WinMopac 2003).

both structures. The MS spectra detected the formation of other oligomers. With the time, however, the formation of very complex, due to the *ortho* and *para* substitution, dendrimeric polymers is quite possible, because the oligomers can react with monomers or with each other if an excess of the strong base is used, i.e. that these oligomers are so-called living polymers. The exemplary calculated dendrimer with statistical distribution of *ortho* and *para* substitutions is shown in Scheme 6.

4. Conclusions

Because of high acidity of the C–H hydrogen atoms ($pK_a = 15.8$; DMSO [33]) in PFPA molecule an addition of a strong N-base causes its deprotonation with formation of a carbanion. The carbanions attack a carbon atom in the aromatic ring in *ortho* or *para* positions of PFPA second molecule with the formation of Meisenheimer complexes and a further elimination F^- anion, which form a hydrogen bonded complex with a protonated MTBD molecule. First, the reaction yields the dimers and with the time also oligomers. The formation of such compounds is confirmed by the high-resolution LSIMS spectra. The FT-IR spectra indicate the formation of carbanions, protonated MTBD molecules as well as the abstraction of the F^- anion in the reaction with formation of asymmetrical intermolecular hydrogen bonds. The structures of **1–2** compounds are confirmed by ^{19}F NMR spectra and visualized by PM5 semiempirical calculations. It is interesting to note that the use of the TBD or MTBD in the reactions with PFPA yield products different from those observed in the reaction of PFPA and NaOH in water/ CCl_4 mixture discussed previously by Nakayama et al. [33].

References

- [1] P. Kirsch, Modern Fluorineorganic Chemistry, Wiley–VCH, Oxford, 2004.
- [2] R.D. Chambers, Fluorine in Organic Chemistry, Blackwell Publishing, New York, 2004.
- [3] G. Schroeder, B. Łęska, A. Jarczewski, B. Nowak-Wydra, B. Brzezinski, J. Mol. Struct. 344 (1995) 77.
- [4] R. Schwesinger, J. Willaredt, H. Schlemper, M. Keller, D. Schmitt, H. Fritz, Chem. Ber. 127 (1994) 2435.
- [5] R. Schwesinger, Nachr. Chem. Tech. Lab. 38 (1990) 1214.
- [6] T. Pietzonka, D. Seebach, Chem. Ber. 124 (1990) 1837.
- [7] H.-J. Gais, J. Vollhardt, C. Krüger, Angew. Chem. 100 (1988) 108.
- [8] M. Fletschinger, B. Zipperer, H. Fritz, H. Prinzbach, Tetrahedron Lett. 28 (1987) 2517.
- [9] B. Brzezinski, G. Schroeder, E. Grech, Z. Malarski, M. Rospenk, L. Sobczyk, J. Chem. Res., Synop. 151 (1997); J. Chem. Res. (M) 1021 (1997)
- [10] B. Brzezinski, P. Radziejewski, G. Zundel, J. Chem. Soc., Faraday Trans. 91 (1995) 3141.
- [11] B. Brzezinski, G. Zundel, J. Mol. Struct. 380 (1996) 195.
- [12] G. Wojciechowski, G. Schroeder, G. Zundel, B. Brzezinski, J. Phys. Chem. A 104 (2000) 7469.
- [13] B. Brzezinski, G. Wojciechowski, F. Bartl, G. Zundel, J. Mol. Struct. 554 (2000) 245.
- [14] B. Brzezinski, G. Wojciechowski, G. Zundel, L. Sobczyk, E. Grech, J. Mol. Struct. 508 (1999) 175.
- [15] B. Brzezinski, G. Zundel, J. Mol. Struct. 446 (1998) 199.
- [16] B. Brzezinski, R. Bauer, G. Zundel, J. Mol. Struct. 436–437 (1997) 297.
- [17] G. Schroeder, B. Łęska, F. Bartl, B. Różalski, B. Brzezinski, J. Mol. Struct. 478 (1999) 255.
- [18] G. Schroeder, B. Łęska, B. Gierczyk, B. Różalski, B. Brzezinski, J. Mol. Struct. 476 (1999) 173.
- [19] G. Schroeder, B. Brzezinski, A. Jarczewski, E. Grech, J. Nowicka-Scheibe, J. Mol. Struct. 344 (1995) 89.
- [20] W. Gałżowski, A. Jarczewski, M. Stańczyk, B. Brzezinski, F. Bartl, G. Zundel, J. Chem. Soc., Faraday Trans. 93 (1997) 2515.
- [21] G. Wojciechowski, B. Brzezinski, J. Mol. Struct. 607 (2002) 111.
- [22] G. Wojciechowski, B. Brzezinski, J. Mol. Struct. 607 (2002) 149.
- [23] G. Wojciechowski, B. Brzezinski, P. Naumov, S. Chantrapromma, A.R. Ibrahim, H.-K. Fun, S.W. Ng, J. Mol. Struct. 598 (2001) 153.
- [24] S.W. Ng, P. Naumov, S. Chantrapromma, S.S.S. Raj, H.-K. Fun, A.R. Ibrahim, G. Wojciechowski, B. Brzezinski, J. Mol. Struct. 569 (2001) 139.
- [25] S.W. Ng, S. Chantrapromma, S.S.S. Raj, H.-K. Fun, A.R. Ibrahim, G. Wojciechowski, B. Brzezinski, J. Mol. Struct. 562 (2001) 185.
- [26] B. Gierczyk, G. Wojciechowski, B. Brzezinski, E. Grech, G. Schroeder, J. Phys. Org. Chem. 14 (2001) 1.
- [27] B. Gierczyk, G. Schroeder, B. Brzezinski, J. Org. Chem. 68 (2003) 3139.
- [28] B. Gierczyk, K. Eitner, G. Schroeder, B. Brzezinski, Pol. J. Chem. 77 (2003) 1437.
- [29] G. Schroeder, K. Eitner, B. Gierczyk, B. Różalski, B. Brzezinski, J. Mol. Struct. 478 (1999) 243.
- [30] J.J.P. Stewart, Methods J. Comput. Chem. 10 (1989) 209.
- [31] J.J.P. Stewart, Methods J. Comput. Chem. 12 (1991) 320.
- [32] P. Przybylski, G. Wojciechowski, B. Brzezinski, G. Zundel, F. Bartl, J. Mol. Struct. 661–662 (2003) 171.
- [33] Y. Nakayama, K. Inukai, K. Hayashi, M. Irik, Bull. Chem. Soc. Jpn 64 (1991) 1226.